

## Fabrication and Experiment of Micro Particle Manipulator

朴宰亨\* · 金容權\*\*

(Jae-Hyoung Park · Yong-Kweon Kim)

**Abstract** - A micro particle manipulator, which is devised for trapping particles at fixed positions by negative dielectrophoretic force (DEP force), has been fabricated and experimented. It is composed of square type electrode arrays fabricated by nickel electroplating with the height of 28  $\mu\text{m}$ . To improve the quality of electroplated nickel electrodes, plating conditions have been optimized. Micro particles used in this study are polystyrene spheres and their diameter is 25  $\mu\text{m}$ . When an alternating electric field is applied to the electrode arrays, polystyrene particles are directed to the specific position and trapped. The DEP force along the moving path of the particles has been estimated by the motion equation of a single particle. The displacement of a particle with an elapsed time was measured using a high-speed camera (1000 frames/sec). The velocity and acceleration of the particle were calculated from the measured data. The DEP force acting on the particle was estimated.

**Key Words** : micro particle manipulator, dielectrophoretic force(DEP force), nickel electroplating, polystyrene spheres

### 1. Introduction

As micromachining technology is improved, it is applied to various fields, and the biotechnology is one of its important applications. Increasing efforts are being made to apply the micromachining technology to the development of micro-devices related to the biotechnology. There are many advantages of the micromachining technology when it is applied to biotechnology such as having comparable dimension with the objects and enabling individual manipulation of the object. Because of a small gap between the electrodes, it is possible to generate sufficient electric field at low electrode voltage. The problem of heating and convection in conductive media can be reduced because of tiny electrodes and low applied voltage.

Since it is required to manipulate the hundred  $\mu\text{m}$  to nanometer ranged particles, the tools with comparable dimension are required. There are many driving forces to manipulate the micro particles. Hydraulic pressure, mechanical force and the dielectrophoretic force (DEP force) can be used for driving the particles. Micropipette was developed to grab and to position a micro particle using hydraulic pressure [1], and the microgripper uses

the mechanical force to manipulate the particle [2]. In these cases, the devices are mechanically contacted with the particles and the particles can be damaged. Compared with these devices, the manipulator using the DEP force has several advantages. It is a non-contact method, so the damage of particle can be reduced. It is more effective to manipulate, to separate, to transport and to characterize a particle and can also be easily fabricated by the micromachining technology. Many research activities are directed towards the fabrication of the particle manipulator using DEP force such as particle separator, particle transport, characterization of a particle, and so on [3-7]. The research presented in this paper is also about the micro particle manipulator using DEP force. The structures fabricated in this paper were devised for trapping particles at a fixed position by negative DEP force. This is the first step towards the realization of nano-scale particle manipulation [8, 9].

The purpose of this paper is to develop the method for the evaluation of DEP force acting on a single particle in the particle trapping system. In previous researches, the design and analysis of micro particle manipulator have been mostly focused on group movement of the particles like the efficiency of transportation or of separation of the particles. However, it is required to manipulate the particle individually in many applications. Therefore, the analysis of the DEP force acting on a single particle is very important in the various particle manipulation systems. In the paper,

\* 正會員 : 서울대 電氣工學部 博士課程

\*\* 正會員 : 서울대 電氣工學部 副教授 · 工博

接受日字 : 2000年 10月 19日

最終完了 : 2001年 3月 3日

experimental measurement of the DEP force acting on a single particle is described for a particle trapping system.

## 2. Theory

DEP (Dielectrophoresis) is one of the various driving forces for the manipulation of micro particles. Dielectrophoresis is the transitional motion of neutral matter caused by polarization effects in a non-uniform electric field [10-12]. By dielectrophoretic force, dielectric particle moves toward the strongest (positive DEP) or to the weakest (negative DEP) electric field region. The DEP force is shown in equation (1) [10].

$$F_{DEP} = \frac{1}{3} \pi r^3 \epsilon_1 \operatorname{Re}[\chi_{eff}] |\nabla E|^2 \quad (1)$$

$r$ : radius of particle

$\epsilon_1$ : permittivity of suspension

$\chi_{eff}$ : effective polarizability of a particle

As shown in equation (1), the sign of effective polarizability, which depends on the frequency of the applied voltage, determines the direction of DEP force. If the sign is negative, the negative DEP force is exerted on the particle, and if the sign is positive, the positive DEP force is generated. The DEP force is proportional to the gradient of square of the applied electric field, which is determined by the geometry of electrodes and the insulator. These characteristics of DEP force are applied to the various particle manipulation systems. We can control the motion of particles by using the corresponding electrode structures depending on the specific purpose. For Example, the particles can be transported to the specific position, and the particles with different electric properties can be separated using positive or negative DEP force. By analyzing the DEP force acting on a particle, we can also characterize the electric property of the particle.

## 3. Design and fabrication

The particle manipulator described in this paper was designed and fabricated for trapping particles at fixed positions. Fig. 1 shows the schematic view of the micro particle manipulator. The particle manipulator is composed of square type electrodes, which are connected with the address lines. When the alternating AC electric fields are applied to these electrodes, the DEP force is acted on the dielectric particle. By the geometry of the electrode structures, the electric field is the weakest at the center among four electrodes. Therefore, the particles are

trapped at that position. The width of the square-type electrodes is  $60 \mu\text{m}$ , and the height of the structures is  $28 \mu\text{m}$ . To reduce the effect of metal address lines in the particle manipulation, the lines were covered with  $1 \mu\text{m}$  thick insulating layer. The space between the electrode is  $60 \mu\text{m}$ , and the width of address line is  $25 \mu\text{m}$ .

Fig. 2 shows the fabrication process of the micro particle manipulator. At first, 200 Å titanium and 1000 Å gold were thermally evaporated on the silicon oxide substrate, respectively and patterned for seed layer and address line (Fig. 2 (a), (b)). And then the  $1 \mu\text{m}$  dielectric layer was coated and patterned. Photoresist was used as an insulator (Fig. 2 (c)). For the stabilization of the dielectric layer, the photoresist should be thermally cured at  $120^\circ\text{C}$  for 60 minutes,  $150^\circ\text{C}$  for 30 minutes and  $200^\circ\text{C}$  for 30 minutes (Fig. 2 (d)). Next thick photoresist (PMER P-LA900PM, TOK. CO. LTD) was coated and patterned by UV-lithography to form an electroplating mold (Fig. 2 (e)). The desired structures were fabricated by electroplating process and removing the mold (Fig. 2 (f)). Finally, the sample was packaged (Fig. 2 (g)). In the fabrication of this micro particle manipulator, the nickel electroplating process is very important because the uniform electrode structures are required for the proper manipulation of the particles. Electroplating is a surface micromachining technology to fabricate microstructures with high aspect ratio and used in many applications because of its simplicity and low cost [13,14]. The electroplating condition should be more carefully controlled in the fabrication of microstructures than the usual electroplating process of a large area. Therefore, the electroplating condition in micro pattern has been optimized. To examine the results of nickel electroplating in micro patterns, arrays of square structures with widths of 10, 15, 25, 30 and  $40 \mu\text{m}$  respectively have been fabricated. Other microstructures with various shapes and widths were also fabricated by electroplating of nickel. To stabilize the current density during the electroplating process, dummy electrode with  $1 \text{ cm}^2$  area was included, and the total size of sample was  $1.7 \text{ cm} \times 1 \text{ cm}$ .

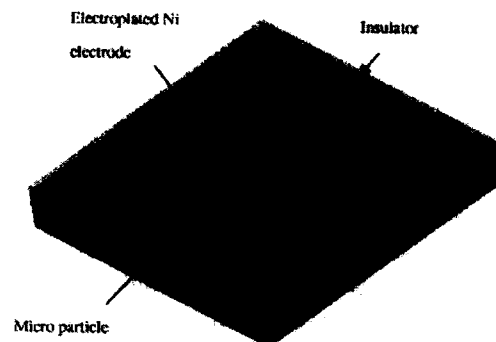


Fig. 1 Schematic view of micro particle manipulator

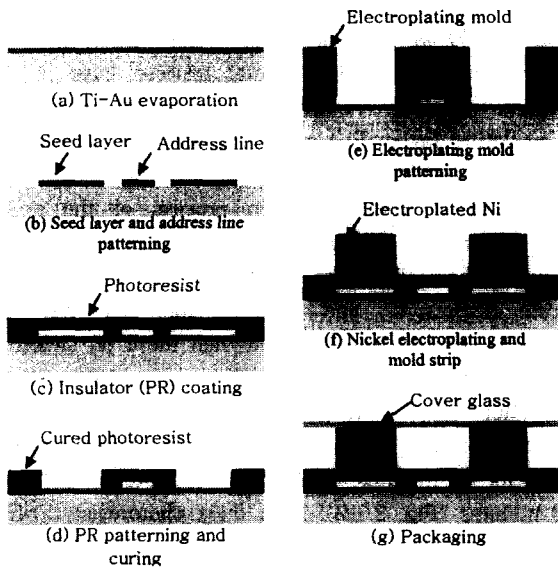


Fig. 2 Fabrication process

Prior to electroplating, the sample should be treated in ultrasonically vibrating electrolytic solution to remove the entrapped air in the electroplating mold. The entrapped air generates traces of bubble shape in electroplated structures and disturbs the uniformity. Therefore, it is important to remove the entrapped air for the purpose of improving the quality of the electroplated structures. Electroplating was carried out using a commercially available nickel sulfamate bath, and the electrolytic solution temperature is fixed at 50 °C. Sulfamate bath requires more careful control than Watts bath. It is much more soluble than the sulfate bath, and it is possible to obtain very high deposition rates by use of a concentrated nickel sulfamate solution. Besides these advantages, electroplated metallic structures using nickel sulfamate bath have low internal stress, so the sulfamate baths are increasingly used for electroforming in micromachining technology [15]. Fig. 3 shows the schematic view of the electroplating system. As shown in Fig. 3, sphere-type nickel meshes enveloped by a titanium basket are used as an anode. The electrolytic solution was mechanically stirred at the speed of 4.5 cm/sec in the process of electroplating with 3 mm gap between the sample and the stirrer. The composition of the electrolytic solution is shown in Table 1. To prevent appearance of pit hole in the electroplated structures, the antipitting agent, which does not appreciably affect the stress of the plate, is added in the electrolyte.

The surface roughness of electroplated structure is improved by mechanical stirring of electrolytic solution and addition of brightener (saccharin). The surface roughness was measured with a non-contact laser surface profiler (KEYENCE VF-7510) and the measured surface roughness(Ra) is  $0.024 \pm 0.007 \mu\text{m}$ . Arrays of

square structures with various pattern sizes have been fabricated to examine the thickness uniformity of electroplated structures. As an example, when the current density is 10 mA/cm<sup>2</sup>, the average electroplating thickness was  $15.41 \pm 0.42 \mu\text{m}$ . When the current densities are 5 and 2 mA/cm<sup>2</sup>, the average thickness of nickel structures was  $7.47 \pm 0.16 \mu\text{m}$  and  $3.62 \pm 0.07 \mu\text{m}$ , respectively. The electroplating rate of nickel was measured with respect to the pattern size and to the current density. As shown in Fig. 4, the electroplating rate is proportional to the current density and the electroplating time regardless of pattern sizes. From the measured data, the thickness of electroplated structures can be controlled by the electroplating time at the fixed current density. From the established electroplating conditions, we could obtain uniform electrode structures that are used in the micro particle manipulator. The fabricated micro particle manipulator is shown in Fig. 5. The thickness of the electroplated nickel electrode is 28  $\mu\text{m}$ .

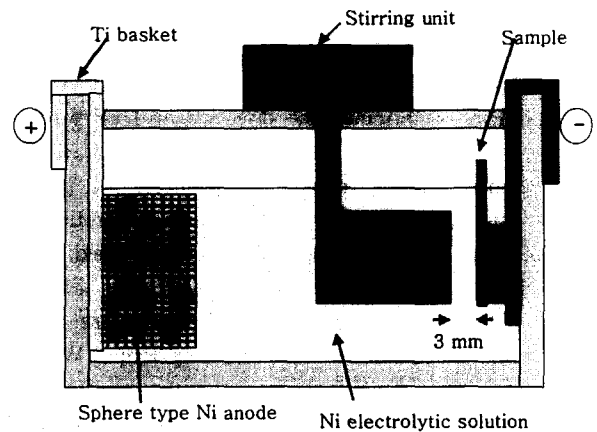


Fig. 3 Schematic view of electroplating system

Table 1 Composition of electrolytic solution

Component	Quantity
Ni(SO <sub>3</sub> NH <sub>2</sub> ) <sub>2</sub> · 4H <sub>2</sub> O	600 g/l
NiCl <sub>2</sub> · 6H <sub>2</sub> O	5 g/l
H <sub>3</sub> BO <sub>3</sub>	45 g/l
Antipitting agent(NP-A)	2 ml/l
Brightener(saccharin)	2 g/l

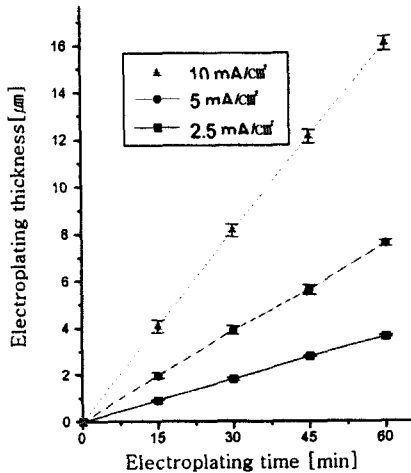


Fig. 4 Electroplating thickness with electroplating time and different current densities



Fig. 5 Fabricated micro particle manipulator

#### 4. Measurement of DEP force

Fig. 6 shows the particle movement when an alternating electric field is applied to the electrodes. The particles used in the experiment are polystyrene spheres with 25 μm in diameter, and are suspended in DI water. In this case the particle moves towards the region of the weakest electric field by negative DEP force. Therefore, the particles are trapped in the center of electrodes as shown in Fig. 7. The applied voltage range was from 2 V<sub>p-p</sub> to 10 V<sub>p-p</sub> and the frequency of the applied voltage was varied from 10 kHz to 10 MHz.

The DEP force acting on a particle can be estimated by the motion equation of a particle suspended in a viscous suspension. The motion equation of a particle that moves under the influence of DEP force in viscous suspension is shown in equation (2) [16]. As shown in equation (2), the total force ( $F_{tot}$ ) exerted on a particle is the sum of the DEP force ( $F_{DEP}$ ) generated by the non-uniformity of the applied electric field and the drag force ( $F_{drag}$ ). The viscosity of suspension influences the

movement of a particle, and the drag force is always exerted in the opposite direction of the particle movement.

$$F_{tot} = F_{DEP} - F_{drag}$$

$$F_{DEP} = F_{tot} + F_{drag} = ma + 6\pi\eta ru = \frac{4}{3}\pi r^3 \rho a + 6\pi\eta ru \quad (2)$$

- $r$  : radius of a particle
- $\rho$  : volume density of a particle
- $u$  : velocity of a particle
- $a$  : acceleration of a particle
- $\eta$  : viscosity of suspension

If we can determine the total force and the drag force, we can get the value of DEP force from equation (2). As shown in equation (2), the velocity and the acceleration of a moving particle should be determined to evaluate the total force and the drag force. The velocity and acceleration of a particle can be calculated from the displacement of a particle with an elapsed time. Therefore, the displacement of a particle and elapsed time is measured along the moving path of a particle as shown in Fig. 7. Along the line of moving path, the particle moves along the x direction because of the symmetry of the electrodes. The motion of a particle was recorded with a high-speed camera, which can take 1000 frames per second. Fig. 8 shows the movement of a particle taken by the high speed camera. From the initial state, the particle moved to the center of electrode arrays with the time. From the measured displacement, the velocity and acceleration of the particle are calculated, and the DEP force can be estimated.

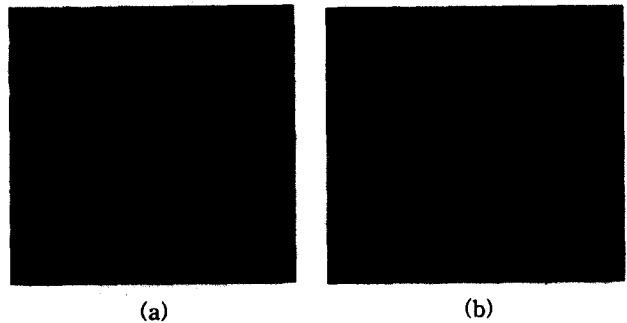


Fig. 6 Micro polystyrene particles in initial state (a) and trapped micro particles (b)

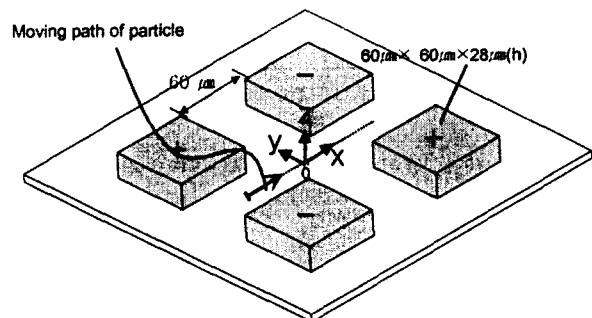


Fig. 7 Schematic view of the moving path of particle

A plot of the particle displacement with elapsed time is shown in Fig. 9. The measured points were fitted with 7th order polynomial, which is represented by the solid line in Fig. 9. By differentiating this fitted function,  $(x(t))$ , we can obtain the velocity function  $(u(t))$ . The acceleration  $(a(t))$  of a particle can also be obtained by differentiating the velocity. From the functions, the DEP force acted on a single particle can be estimated by equation (2). In this case, the radius and volume density of a particle are  $12.5 \mu\text{m}$  and  $1040 \text{ kg/m}^3$ , respectively. The viscosity of suspension is  $10^{-3} \text{ kg/m} \cdot \text{sec}$ . Fig. 10 shows the estimated DEP force with variable applying voltages and frequencies. As shown in Fig. 10 (a), the DEP force increases when the applied voltage increases from 5 to 7 and to 10 Vpp. Also, the DEP force is varied with the frequency as shown in Fig. 10 (b), which is explained by the effective polarizability term in equation (1) depending on the applied frequency.

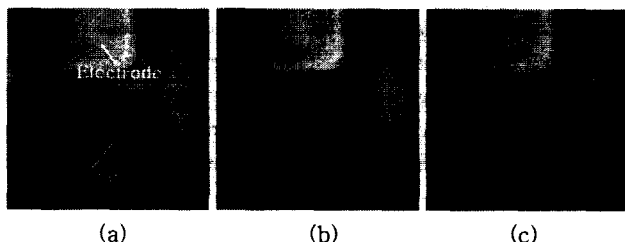


Fig. 8 Movement of a particle with elapsed time taken by high-speed camera for the measurement of displacement (a) Before applying voltage, (b) 0.2 second after and (c) 0.6 second after

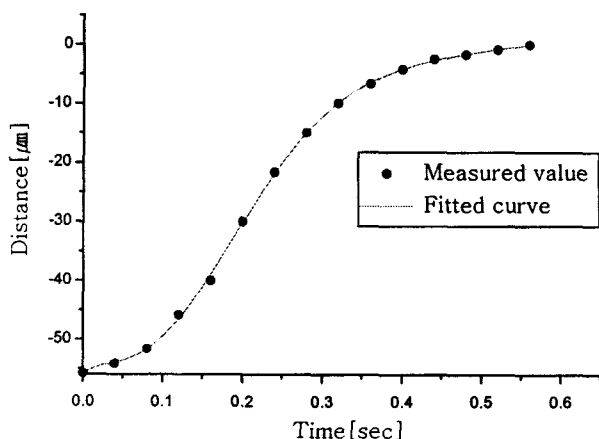
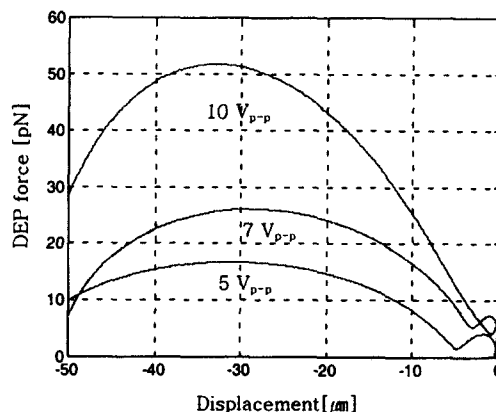
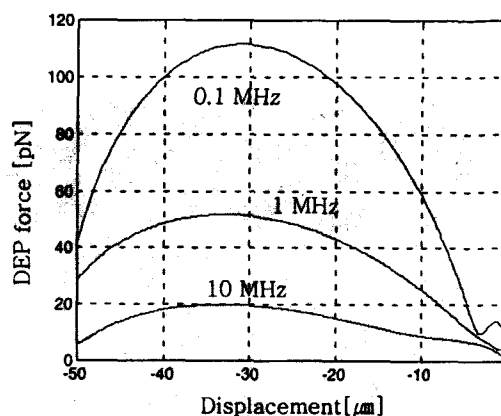


Fig. 9. The displacement of particle with elapsed time and fitted curve



(a)



(b)

Fig. 10 DEP force (a) with applied voltages at the frequency of 1 MHz and (b) with variable frequencies at 10 V<sub>p-p</sub> applied voltage

### 5. Discussion

To verify the experimental results, the DEP force has been computed using FEM package program, Maxwell. Simulated result was compared with the experimental result in the case that the applied voltage is 10 V<sub>p-p</sub> and the frequency is 0.1 MHz. The dimension of the electrode arrays used in the simulation is identical to the fabricated electrode arrays. Table 2 shows the electrical constants of a polystyrene particle and the suspending medium, which were used in the calculation of DEP force.

The equation (1) is induced from the dipole approximation for the force exerted upon any physical dipole, such as a polarized particle of finite size. The dielectrophoretic approximation is usually adequate for the case that the dimensions of electrodes are much larger than the particles. However, the diameter of the particle used in the paper is  $25 \mu\text{m}$ , and the gap between electrodes is  $60 \mu\text{m}$ , so the dimension of this model is not consistent with the dielectrophoretic approximation.

Therefore, higher order moment of a particle should be considered for more accurate analysis. In this paper, the quadrupole moment of a particle was added to the calculation of the DEP force. Equation (3) can be used to calculate the force contributed by the quadrupole moment of a particle.

$$F_{quadrupole} = \frac{1}{3} \pi r^5 \epsilon_1 \text{Re}[K^{(2)}] \nabla[\nabla \bar{E} : \nabla \bar{E}] \quad (3)$$

r: radius of particle

$\epsilon_1$ : permittivity of suspension

$K^{(2)}$ : polarization coefficient for quadrupole moment

Dyadic notation is employed to represent the tensor nature of the higher order multipoles [17]. In equation (4),  $\nabla \bar{E} : \nabla \bar{E}$  is expressed according to the double dot operation.

$$\nabla \bar{E} : \nabla \bar{E} = \left(\frac{\partial E_x}{\partial x}\right)^2 + \left(\frac{\partial E_y}{\partial y}\right)^2 + \left(\frac{\partial E_z}{\partial z}\right)^2 + 2\left(\frac{\partial E_x}{\partial x} \cdot \frac{\partial E_x}{\partial y}\right) + 2\left(\frac{\partial E_x}{\partial y} \cdot \frac{\partial E_y}{\partial z}\right) + 2\left(\frac{\partial E_x}{\partial z} \cdot \frac{\partial E_z}{\partial x}\right) \quad (4)$$

The total force exerted on the particle in a nonuniform electric field is sum of the dipole moment and the quadrupole moment terms as shown in equation (5).

$$F_{total} = F_{dipole} + F_{quadrupole} = \pi r^3 \epsilon_1 \text{Re}[K] |\nabla \bar{E}|^2 + \frac{1}{3} \pi r^5 \epsilon_1 \text{Re}[K^{(2)}] \nabla[\nabla \bar{E} : \nabla \bar{E}] \quad (5)$$

The DEP force has been computed by using equation (4) and (5). The simulated result using equation (5) is shown in Fig. 11. As shown in Fig. 11, the simulated value is about twice higher than the experimented values. The most prospective reason for the difference between the experiment and the simulation results is the effect of the adhesive force of a particle to a bottom surface. When a charged dielectric particle is immersed in a fluid and rested on a planar dielectric surface, it experiences a net electrostatic adhesion force [12]. The adhesion force is not considered in the experimental estimation of the DEP force. This effect results in underestimation of the DEP force evaluated by the experiment. In this case, the image force contribution is the dominant adhesive force. The image force is produced due to the induced image charges of the dielectric surface and close proximity to a conductor, so it can be reduced by increasing the thickness of the insulator [4]. With the adhesive force considered, we can analyze the DEP force more accurately. Another reason of difference between experiment and simulation results is that a particle does

not move straight along the moving path but moves in rotational and translational motion in other directions. The difference is also due to the effects of surface friction, heating and convection of the suspending medium, so for more accurate analysis, these effects should be considered. Despite of the difference between simulated result and experimental result, the tendency of force distribution is very similar. Therefore, the method for determining the DEP force studied in this paper can be applied to the design and the analysis of the various particle manipulation systems.

Table 2 Electrical constants of polystyrene particle and suspending medium

Parameter	Value
r	$1.25 \times 10^{-5}$ [m]
$\epsilon_1$	$7.083 \times 10^{-10}$ [F/m]
$\epsilon_2$	$2.302 \times 10^{-11}$ [F/m]
$\sigma_1$	$5.882 \times 10^{-6}$ [S/m]
$\sigma_2$	10-19 [S/m]

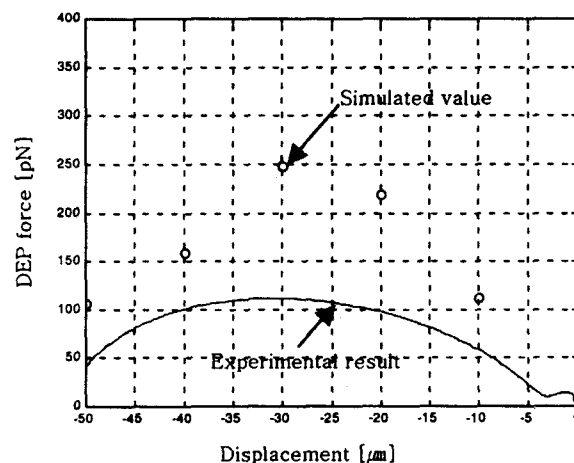


Fig. 11 Comparison of DEP force from experiment and FEM analysis

### 6. Conclusions

In this paper, a micro particle manipulator, which can trap the particles at fixed points, was fabricated and the DEP force acting on a particle was estimated. The electroplated nickel electrodes with the comparable height to the particle size were used to generate nonuniform electric fields. By optimizing the various electroplating conditions, nickel electrodes have been fabricated uniformly.

When the alternating electric field is applied to the electrodes, the particles move toward the weakest electric field region by the negative DEP force. The DEP force

acting on a particle was determined experimentally by the motion of a particle in electrode arrays. As shown in experimental results, the DEP force increases when the applied voltage increases. Also, the DEP force was varied with frequency. The experimental results were compared with the simulated value by FEM analysis. In the FEM simulation, the quadrupole moment of a particle was added to the dipole term in the calculation of DEP force, because the dimension of experiment model was not consistent with the dielectrophoretic approximation. The simulated value is about twice higher than the experimented values, but the tendency of force distribution is very similar.

A micro particle manipulator studied in this paper can be used in many applications to manipulate particles and biological cells. Various particle manipulation systems can be designed on the basis of established fabrication technique and method for analyzing the DEP force presented in the paper. One of the applications using this technique is the particle separator. Using the positive and negative DEP force, particles with different electric property can be separated with an applied electric field. Other possible applications are the particle transportation, arrangement of particles into groups for observation of individual particles and characterization of particles.

#### Acknowledgement

This research was supported by Nano Bioelectronics & Systems Research Center.

#### References

- [1] H. Aoyama, S. Hiraiwa, F. Iwata, F. Fukaya, and A. Sasaki, Miniature robot with micro capillary capturing probe, *Proc. 6th Int. Symp. on Micro Machine and Human Science*, pp. 173-178, 1995.
- [2] C. -J. Kim and A. P. Pisano, Silicon-processed overhanging microgripper, *J. Microelectromech. Syst.*, Vol. 1, No. 1, pp. 31-36, 1992.
- [3] H. Morgan, N. G. Green, M. P. Hughes, W. Monaghan, and T. C. Tan, Large-area travelling-wave dielectrophoresis particle separator, *J. Micromech. Microeng.*, Vol. 7, pp. 65-70, 1997.
- [4] A. Desai, S. W. Lee, and Y. C. Tai, A MEMS electrostatic particle transportation system, *Proc. IEEE Micro Electro Mechanical Systems*, pp. 121-126, 1998.
- [5] N. G. Green, and H. Morgan, Dielectrophoretic separation of nano-particles, *J. Phys. D: Appl. Phys.*, Vol. 30, pp. L41-L44, 1997.
- [6] M. Washizu, Manipulation of biological objects in micromachined structures, *Proc. IEEE Micro Electro Mechanical Systems*, pp. 196-201, 1992.
- [7] X-B. Wang, Y. Huang, J. P. H. Brut, G. H. Markx, and R. Pethig, Selective dielectrophoretic confinement of bioparticles in potential energy wells, *J. Phys. D: Appl. Phys.*, Vol. 26, pp. 1278-1285, 1993.
- [8] G. Fuhr, W. M. Arnold, R. Hagedorn, T. Müller, W. Benecke, B. Wagner, and U. Zimmermann, Levitation holding, and rotation of cells within traps made by high-frequency fields, *Biochimica et Biophysica Acta* Vol. 1108, pp. 215-223, 1992.
- [9] T. Schnelle, R. Hagedorn, G. Fuhr, S. Fiedler, and T. Müller, Three-dimensional electric field traps for manipulation of cells-calculation and experimental verification, *Biochimica et Biophysica Acta*, Vol. 1157, pp. 127-140, 1993.
- [10] H. A. Pohl, *Dielectrophoresis*, Cambridge University Press, London, 1978.
- [11] I. Turcu and C. M. Lucaciu, Dielectrophoresis : A Spherical Shell Model, *J. Phys. A: Math. Gen.*, Vol. 22, pp. 985-993, 1989.
- [12] T. B. Jones, *Electromechanics of particles*, Cambridge University Press, New York, 1995.
- [13] A. B. Frazier and M. G. Allen, High Aspect Ratio Electroplated Microstructures Using A Photosensitive Polyimide Process, *Proc. IEEE Micro Electro Mechanical Systems*, pp. 87-92, 1992.
- [14] A. B. Frazier and M. G. Allen, Metallic Microstructures Fabricated Using Photosensitive Polyimide Electroplating Molds, *Journal of Microelectromechanical Systems*, vol. 2, no. 2, pp. 87-94, 1993.
- [15] F. A. Lowenheim, *Modern Electroplating*, John Wiley & Sons, 1974.
- [16] J. H. Choi, Estimation Method of the DEP Force Exerted on a Cell in a Planar Electrode Structure, Master thesis, Seoul National University, Seoul, Korea, 1996.
- [17] R. B. Bird, R. C. Armstrong, and O. Hassager, *Dynamics of polymeric liquids*, John Wiley & Sons, 1977.

저 자 소 개



박재형 (朴宰亨)

1997년 서울대 공대 전기공학부 졸업. 1999년 동대학원 졸업(석사). 1999-현재 동대학원 전기공학부 박사 과정

Tel : 02-888-5027, Fax : 02-873-9953

E-mail : parkjae@chollian.net



김용권 (金容權)

1983년 서울대 공대 전기공학과 졸업. 1985년 동대학원 졸업(석사). 1990년 동경대 대학원 졸업(공학). 1990년 히다찌 중앙 연구소 연구원. 1992년-현재 서울대 전기공학부 교수

Tel : 02-880-7440, Fax : 02-873-9953

E-Mail : yongkim@chollian.net